Ab initio study of the $O(^1D)+CH_4(X\,^1A_1)\rightarrow OH(X\,^2\Pi)+CH_3(X\,^2A_2'')$ reaction: Ground and excited potential energy surfaces

Jordi Hernando[a)]
Departament de Química Física i Centre Especial de Recerca en Química Teòrica, Universitat de Barcelona i Parc Científic de Barcelona, C/Martí i Franquès, 1, 08028 Barcelona, Spain

Judith Millán
Departamento de Química, Universidad de La Rioja, C/Madre de Dios, 51. 26006 Logroño, Spain

R. Sayós[b)] and Miguel González[c)]
Departament de Química Física i Centre Especial de Recerca en Química Teòrica, Universitat de Barcelona i Parc Científic de Barcelona, C/Martí i Franquès, 1, 08028 Barcelona, Spain

(Received 11 April 2003; accepted 13 August 2003)

The two potential energy surfaces ($1\,^1A$ and $2\,^1A$ PESs) adiabatically correlating the reactants and products asymptotes of the title reaction were studied by means of the CASSCF and CASPT2 *ab initio* methods. The minimum energy path determined for the ground PES evolved through the barrierless insertion of the $O(^1D)$ atom into a C–H bond. The $OH+CH_3$ products result from the dissociation of the CH_3OH methanol intermediate formed. Reactivity on the excited $2\,^1A$ PES was found to proceed via an abstraction pathway. The energy barrier involved is low enough to expect the $2\,^1A$ PES to play a non-negligible role in the title reaction, even at the usual conditions attained in the experiments. The crossing between the $1\,^1A$ and $3\,^1A$ PESs was also investigated, the latter surface correlating with the excited $OH(A\,^2\Sigma^+)$ product. © *2003 American Institute of Physics.* [DOI: 10.1063/1.1615766]

I. INTRODUCTION

The reaction of methane with the oxygen atom in the first excited electronic state,

$$O(^1D)+CH_4(X\,^1A_1)\rightarrow OH(X\,^2\Pi)+CH_3(X\,^2A_2'')$$

$$\Delta H^{\circ}_{298\ K}=-43.1\ \ \text{kcal mol}^{-1}\ \ \text{(Ref.1)}, \qquad (1)$$

is an important source for stratospheric OH, which partly determines the chemistry of the Earth's ozone layer through the HO_x cycles.[2–4] The $OH+CH_3$ reaction channel is the most important one for the $O(^1D)+CH_4$ reaction [quantum yield of 0.75 ± 0.15 at 300 K (Ref. 5)], whose overall rate constant at room temperature approaches the gas kinetic limit: $k=1.5\times10^{-10}$ cm^3 molecule^{-1} s^{-1}.[5]

The dynamics of reaction (1) was extensively studied from an experimental point of view. Laser-induced fluorescence (LIF) and chemiluminescence measurements of the OH nascent internal state distributions were carried out.[6–13] Polarized Doppler-resolved LIF spectroscopy[14–18] was used to study the OH product state-resolved kinetic energy and angular distributions. Very recently, the same properties for the global OH product have been determined using molecular beams.[19] The energy distribution of the CH_3 was also measured.[20,21]

Reaction (1) was also theoretically studied. *Ab initio* calculations were reported for the ground potential energy surface.[22,23] The complete active space self-consistent field (CASSCF) and multireference double configuration interaction (MRDCI) methods were used in Ref. 22, where a quite small active space (six electrons in five orbitals) and a limited basis set (50 basis functions) were considered. On the other hand, we employed the monoreference UMP2 (second-order unrestricted Møller–Plesset) and UMP4 (fourth-order unrestricted Møller–Plesset) methods (and their spin-projected variants PUMP2 and PUMP4, respectively) and a large basis set (116 basis functions) in Ref. 23. The broken symmetry approach was applied in that work due to the multireference character of the $1\,^1A$ PES. Both the aforementioned works concluded that the minimum energy path (MEP) of the $1\,^1A$ PES consisted on a collinear approach of $O(^1D)$ to a C–H bond, which involved a transition state placed 2–3 kcal mol^{-1} above reactants. In Ref. 22 it was stated that, once this barrier is surmounted, the MEP evolved through the off-axis migration of the oxygen atom and its insertion into a C–H bond, yielding the methanol intermediate. However, this statement could not be asserted by the calculations reported in Ref. 23. The *ab initio* data of Ref. 23 were used to derive two versions of a triatomic analytical representation of the $1\,^1A$ PES,[23,24] which were employed in a quasiclassical trajectory (QCT) study of the reaction dynamics.[23–25]

Here, we describe a new *ab initio* study of reaction (1), which focused not only on the description of the ground PES of the system, but also on the characterization of the first excited one ($2\,^1A$ PES), which also adiabatically correlates

a)Present address: Applied Optics Group, Faculty of Applied Physics, University of Twente, P.O. Box 217, 7500 AE Enschede, The Netherlands.
b)Author to whom correspondence should be addressed. Electronic mail: r.sayos@ub.edu
c)Author to whom correspondence should be addressed. Electronic mail: miguel.gonzalez@ub.edu

reactants and products. This study casts some light on those features of the $1\,^1A$ PES that could not be unambiguously described in previous works,[22,23] due to limitations of the *ab initio* methods employed. Moreover, here it was possible to analyze the role of the excited PESs of the system. This problem had previously been extensively considered for the analogous and simpler $O(^1D)+H_2\rightarrow OH+H$ reaction (see, e.g., Refs. 26–32). Finally, the present paper gives some attention to the crossing between the $1\,^1A$ and $3\,^1A$ PESs, the latter correlating with the excited $OH(A\,^2\Sigma^+)$ product.

II. COMPUTATIONAL METHOD

A very important feature of the $O(^1D)+CH_4$ system is its diradical character. It behaves as an open-shell singlet in most regions of the PESs correlating reactants with products, particularly in the entrance [owned to the $O(^1D)$ species] and exit (owned to the $OH+CH_3$ species) zones. Hence, in a qualitatively correct treatment of reaction (1), one must include at least two reference configurations to describe the wave function of the system.[33] Nevertheless, it is possible to relax this requirement and to obtain a quite good description of this system by employing a monoreference method of calculation, provided that a broken symmetry singlet wave function is generated and its energy is projected to avoid spin contamination (cf. Ref. 23). However, some methodological (breaking of the spatial symmetry and accuracy of the projected energies) and practical (neither geometry nor frequencies are usually computed at the projected level) problems occur when employing this approach. Hence, a multireference method is recommended to study this reaction.

In this work we employed the CASSCF and CASPT2 (complete active space, second order perturbation theory) methods. This approach seems to be accurate enough to study reaction (1). The CASSCF method is intended to introduce the main part of the nondynamical correlation energy.[34] The CASPT2 method introduces the dynamical correlation to the CASSCF wave function by computing the energy at the second order of perturbation theory.[35] The CASPT2 method has an estimated error in the exoergicities of ± 2 kcal mol^{-1} for isogyric reactions (i.e., reactions that conserve the number of electron pairs in reactants and products), assuming that the active space includes all the valence electrons and a large enough basis set is used.

The CASPT2 and CASSCF calculations were performed by means of the MOLCAS 4.1 program,[36] which allows the computation of CASSCF energies, analytical gradients, and numerical Hessians, and CASPT2 energies. Unfortunately, neither geometry optimizations nor harmonic vibrational frequency calculations at the CASPT2 level are available in MOLCAS 4.1. Because of this, we usually obtained the optimal geometries and frequencies of the stationary points of reaction (1) at the CASSCF level, and then performed CASPT2 pointwise calculations on the resulting structures (i.e., CASPT2//CASSCF calculations). However, in some particular cases (diatomic molecules and highly symmetric molecules) or when the optimal CASPT2 geometries were found to be significantly shifted with respect to their CASSCF counterparts, numerical optimizations at the CASPT2 level were performed for all or some of the internal degrees of freedom of the analyzed structures.

After several checks, we selected as a suitable active space for the CASSCF calculations the one denoted as (14, 12) (i.e., 14 active electrons distributed in 12 active orbitals with the appropriate symmetry and spin). This full valence active space leads to about 84 300 configuration state functions. When applying the CASPT2 method, the correlation energy was only computed for the valence electrons (frozen-core approach). In addition, the G2 variant of the CASPT2 method was used, as it produces a balanced treatment of both open- and closed-shell configurations. In the CASPT2 calculations, it was checked that the weight of the reference CASSCF wave function was always above 0.90.

To select the set of basis functions to be employed, two different basis sets were tested by calculating the exothermicity of reaction (1) and the dissociation energy of the CH_3OH minimum (methanol molecule) of the $1\,^1A$ PES: the 6-311G($2df$,$2pd$) basis set of Pople[37] (116 basis functions) and the cc-pVTZ basis set of Dunning[38] (116 basis functions). Since both basis sets yielded very similar results (differences of 1 kcal mol^{-1} or less were observed), the 6-311G($2df$,$2pd$) basis set was chosen, as in Ref. 23. By using such a large basis set, together with the full valence active space, we expected to overcome the main difficulties found in a previous multireference calculation,[22] due to the limited size of the basis set and active space employed in that work.

III. RESULTS

For C_1, C_s, and C_{3v} symmetries, the following PESs correlate with the asymptotic regions of reaction (1) (Fig. 1): (a) reactants: $(5)\,^1A(C_1)$, $(3)\,^1A'+(2)\,^1A''(C_s)$, and $(2)\,^1E+{}^1A_1(C_{3v})$; (b) products: $(2)\,^1A+(2)\,^3A(C_1)$, $^1A'+{}^1A''+{}^3A'+{}^3A''(C_s)$, and $^1E+{}^3E(C_{3v})$. Hence, both asymptotes correlate adiabatically through the following PESs: $(2)\,^1A(C_1)$, $^1A'+{}^1A''(C_s)$ and $^1E(C_{3v})$. As shown in Fig. 1, the ground ^1E PES crosses with the excited $^1A_1$ surface for C_{3v} symmetry, the latter PES correlating with excited products. As a consequence, an avoided crossing exists for geometries close to C_{3v} symmetry between the $1\,^1A$ and $3\,^1A$ PESs ($1\,^1A'$ and $2\,^1A'$ in C_s symmetry). This makes that the ground $1\,^1A$ PES presents $^1A_1$ character in the reactants region and ^1E character in the products region for these geometries, while the $3\,^1A$ PES connecting reactants with excited products shows ^1E and $^1A_1$ characters in the entrance and exit channels, respectively. The $2\,^1A$ PES, which connects reactants with ground products, presents ^1E character for geometries close to C_{3v} symmetry.

This *ab initio* study mainly focused on the two PESs adiabatically correlating the reactants and products of reaction (1): $1\,^1A$ (ground PES) and $2\,^1A$ (excited PES) for C_1 symmetry. The ground PES correlates with the CH_3OH alcohol minimum, as shown in Fig. 1. The accuracy of the *ab initio* methods chosen to characterize these PESs was checked by comparing the calculated values of the reactants and products geometries and harmonic vibrational frequencies, the reaction exothermicity and the dissociation energy of the alcohol minimum with experimental data. Table I sum-

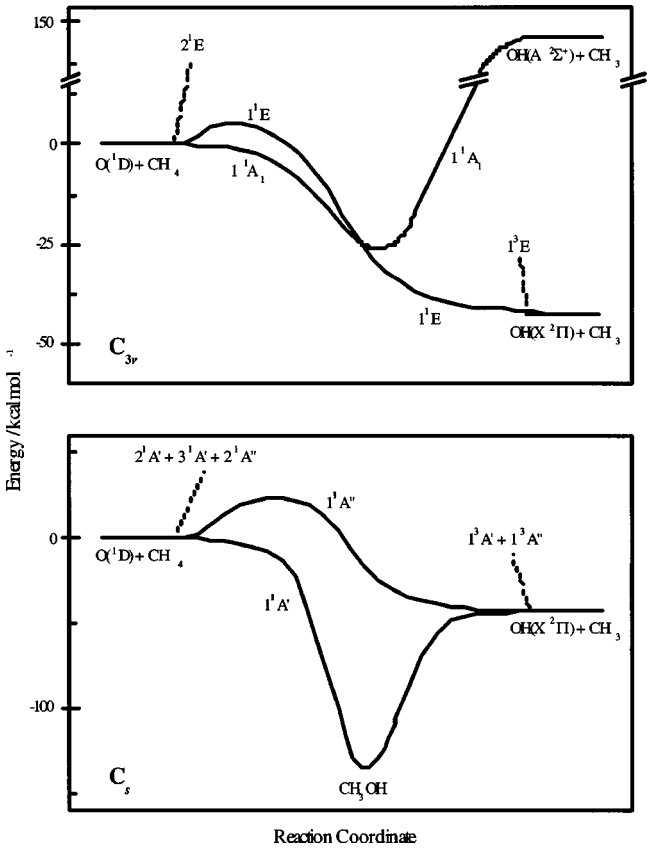

FIG. 1. Schematic representation of the potential energy surfaces of the title reaction under C_{3v} and C_s symmetries.

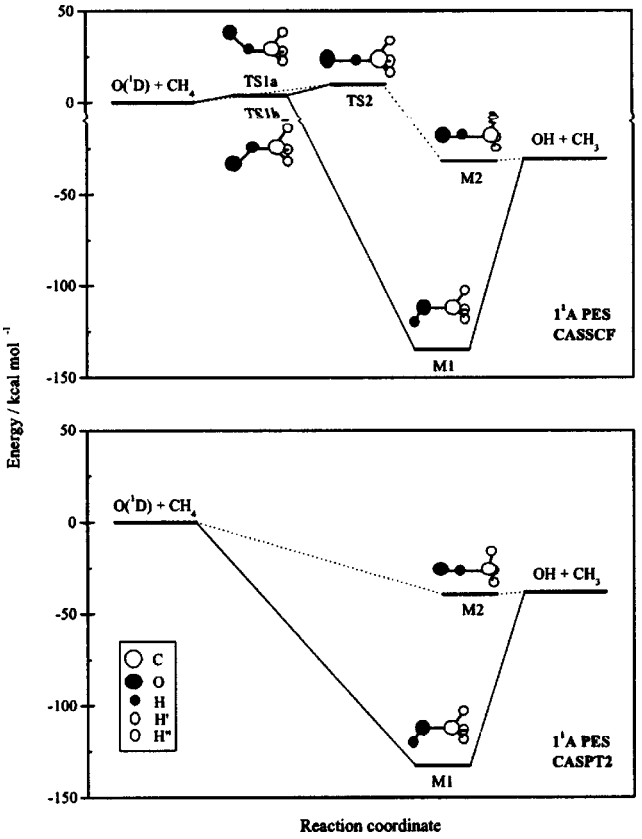

FIG. 2. Schematic representation of the stationary points and connections between them found at the CASSCF and CASPT2 *ab initio* levels for the $1\,^1A$ PES.

marizes the theoretical and experimental results on the energetics of reaction (1) and methanol. The geometries and harmonic frequencies of reactants and products are shown in Table A of the supplementary material.[39]

The CASPT2//CASSCF method properly reproduces the exothermicity of the reaction (less than 2% of relative error). Moreover, the description of the dissociation energy of the methanol minimum is also rather good at this level (less than 5% of relative error). However, the CASSCF method and the PUMP4//UMP2 method used in our previous work of Ref. 23 yield slightly better results for the alcohol specie. This may be explained on the basis of a non-negligible shift between the optimal CASSCF and CASPT2 structures for CH_3OH. As proof, if a CASPT2 pointwise calculation is performed on the UMP2/6-311G($2df$,$2pd$) geometry obtained in Ref. 23, the absolute energy value obtained (-115.50601 H) matches the CASPT2//CASSCF one (-115.50609 H). As the UMP2 and CASSCF geometries for CH_3OH are significantly different (cf. in Table II), it can be assumed that if the CASPT2 energy was computed on the optimal CASPT2 structure, the energy value would be lower and, therefore, the dissociation energy of the minimum larger and closer to the experimental value. Regarding the properties of reactants and products, their geometries and harmonic frequencies are properly reproduced by means of the CASSCF and CASPT2 methods.

TABLE I. Energetics of reaction (1).

Method	$E+$ZPE/kcal mol^{-1} [a]	
	CH_3OH minimum	CH_3+OH
CASSCF/6-311G($2df$,$2pd$)	-129.4 (-134.8)	-34.8 (-30.4)
CASPT2//CASSCF/6-311G($2df$,$2pd$)	-127.5 (-132.9)	-42.7 (-38.3)
PUMP4//UMP2/6-311G($2df$,$2pd$)[b]	-129.2 (-133.5)	-42.6 (-38.6)
MRCI//CASSCF[c]	-122.2 (-125.8)	-42.5 (-38.2)
Experimental data[d]	-133.9	-43.5

[a]Energy referred to reactants. The values in parentheses correspond to the energies without including the zero point energies.
[b]Reference 23.
[c]Reference 22. A (6,5) active space and a split-valence $(9s5p)/[3s2p]$ basis set of Huzinaga–Dunning–Raffenetti plus d polarization functions for C and O and p polarization function for H atoms were used.
[d]$\Delta H^\circ_{0\,\mathrm{K}}$ from Ref. 1.

A. Ground $1\,^1A$ PES

A preliminary search of the stationary points occurring on the ground $1\,^1A$ PES was performed using the CASSCF method, since gradients (analytical) and Hessians (numerical) can be computed at this level. The connections between the stationary points found and the reactants and products asymptotes were also studied by carrying out relaxed scans along proper reaction coordinates (Fig. 2 and Table II, and Table B in the supplementary material[39]).

The CASSCF MEP on the $1\,^1A$ PES proceeds via a noncollinear attack of the O(^1D) atom to a C–H bond, leading to an early transition state (TS) with the O, H, C, and H′ atoms placed in the same plane (Fig. 2). Two different struc-

TABLE II. Properties of the stationary points of the 1 ^1A and 2 ^1A PESs.[a,b]

Stationary point	R_{OH}/Å	R_{HC}/Å	$R_{H'C}$/Å	$R_{H''C}$/Å	∠CHO/°	∠H′CH/°	∠H″CH/°	∠H′CHO/°	E+ZPE/kcal mol^{-1}
1 ^1A									
TS1a/TS1b									
CASSCF ($^1A'$)									
TS1a	1.638	1.123	1.097	1.101	124.5	111.8	106.8	0.0	3.6 (3.8)
TS1b	1.638	1.123	1.102	1.098	124.5	105.3	109.9	180.0	3.6 (3.8)
CASPT2//CASSCF									
TS1a/TS1b									−3.3 (−3.1)
PUMP4 ($^1A'$)[c]	1.513	1.140	1.083	1.083	179.9	108.2	108.4	0.0	−0.1 (3.6)
MRCI//CASSCF ($^1A_1$)[d]	1.66	1.10	1.08	1.08	180.0	108.7	108.7		(2.1)
Experiment[e]									≈0
M1 ($^1A'$)									
CASPT2//CASSCF	0.9602	1.954	1.102	1.085	44.1	134.3	97.3		−127.5 (−132.9)
PUMP4//UMP2[c]	0.956	1.928	1.085	1.091	44.3	135.2	97.6	0.0	−129.2 (−133.5)
MRCI//CASSCF[d]									−122.2 (−125.8)
Experiment[e]	0.9630	1.9481	1.0937	1.0937	43.9	140.0	96.4	0.0	−133.9
TS2 ($^1A_1$)									
CASSCF	1.446	1.123	1.099	1.099	180.0	107.2	107.2		4.3 (5.8)
CASPT2//CASSCF									−4.9 (−3.4)
M2 (^1E)									
CASSCF	0.9729	2.781	1.092	1.092	180.0	93.8	93.8		0.05 (−1.1)
CASPT2//CASSCF									0.65 (−1.8)
2 ^1A									
TS1′ (^1E)									
CASSCF	1.401	1.208	1.093	1.093	180.0	106.8	106.8		(12.0)
CASPT2//CASSCF									(−1.6)
CASPT2[f]	1.625	1.120	1.097	1.097	180.0	108.9	108.9		(1.2)
M2′ (^1E) (see M2)									

[a]See Fig. 2 for the internal coordinates definition. Energy referred to reactants for TS1a, TS1b, M1, TS2, and TS1′, while referred to products for M2 and M2′. The values in parentheses correspond to the energies without including the zero point energies.
[b]The harmonic vibrational frequencies of the stationary points computed at the CASSCF level are given in Table B of the supplementary data.
[c]Reference 23.
[d]Reference 22.
[e]Reference 5.
[f]The optimal CASPT2 geometry for TS1′ was obtained from a bicubic spline fitting of a set of 24 CASPT2 points computed around the CASSCF structure (see text for further explanation).

tures were distinguished for this TS, depending on whether the O–H–C–H′ dihedral angle was equal to 0° (TS1a) or 180° (TS1b). Both structures are very similar in geometry (except for the aforementioned dihedral angle) and energy (Table II). The energy barrier for these TSs is 3.8 kcal mol^{-1}, which is in agreement with what was reported in Ref. 23 (3.6 kcal mol^{-1}), but higher than the value of Ref. 22 (2.1 kcal mol^{-1}). When including the zero point vibrational energy (ZPE) correction, the energies of TS1a and TS1b remain above reactants (3.6 kcal mol^{-1}). On the other hand, the experiments suggested that reaction (1) should not present activation energy,[5] and this was also proposed in the *ab initio* study of Ref. 23. This suggests that a proper description of this early transition state requires the inclusion of the dynamical correlation energy, as the CASPT2 results shown below demonstrate.

Once the barrier is surmounted, the CASSCF MEP evolves through the insertion of the $O(^1D)$ atom into a C–H bond, reaching the CH_3OH minimum (M1). This means that the MEP is of insertion type. This was also stated in Ref. 22, although the early TS found in that work presented a collinear O–H–C arrangement, instead of the noncollinear one obtained here. The geometry of a TS connecting reactants with CH_3OH should be expected to be bent, since a collinear O–H–C barrier could be thought to lead directly to products (without passing through the alcohol minimum) via an abstraction pathway. Thus, for the related $O(^1D)+H_2$ reaction the MEP connecting reactants with the H_2O minimum occurs via a bent attack of the $O(^1D)$ atom to the H_2 molecule.[40]

An examination of the imaginary frequency and evolution along the intrinsic reaction coordinate for the TS determined in our previous work of Ref. 23 (collinear O–H–C arrangement) indicated that it corresponds to an abstraction type MEP. Such detailed analysis was not performed in Ref. 22 to elucidate the nature of the TS. However, leaving aside whether the early TS found in that work allows for insertion or not, we believe that our present results lead to a better description of this stationary point. The broken symmetry wave function used in Ref. 23 to optimize the TS structure did not stand for the pure singlet state, but for a 50:50 mix of the singlet and triplet states of the system. The active space and basis set employed in Ref. 22 were significantly smaller than those used here. Hence, the CASSCF MEP of reaction

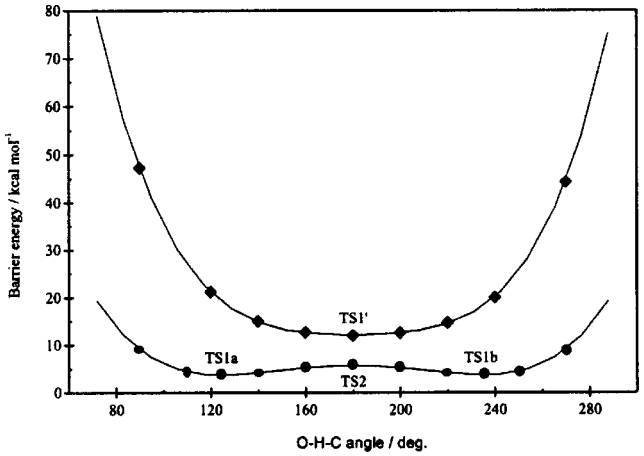

FIG. 3. Dependence of the CASSCF energy barrier with the O–H–C angle for the $1\,^1A$ (●) and $2\,^1A$ (◆) PESs.

(1) corresponds to the insertion of the $O(^1D)$ atom into a C–H bond proceeding via a bent (O–H–C) transition state.

The properties of the CH_3OH minimum are well described at the CASSCF level (Table II). The alcohol minimum connects with products along the MEP without surmounting any energy barrier above them. A similar situation was obtained when analyzing the fragmentation of CH_3OH to produce CH_3O+H, which is another reaction channel of the $O(^1D)+CH_4$ system.[19] These results agree with those reported in Refs. 22 and 23.

The evolution of the energy barrier with the O–H–C attacking angle was also studied at the CASSCF level. We analyzed the approach of oxygen to methane for different angles. To make the calculations easier, they were performed assuming the existence of an O–H–C–H′ planar geometry (i.e., assuming C_s symmetry), in accordance with the fact that the CASSCF MEP of reaction (1) was found to maintain such planar structure. The results obtained are depicted in Fig. 3. The energy barrier was found to be minimal for the TS1a and TS1b structures, which present a deviation with respect to the O–H–C collinear geometry of $\pm 55.5°$. As this deviation increases, the energy barrier rises smoothly. On the other hand, when O–H–C conformations closer to the collinear limit are considered, the energy barrier increases slightly and a maximum is reached (at about 6.0 kcal mol^{-1}) for an O–H–C angle nearly equal to 180°. For this angle, the energy gradient and harmonic frequencies of the structure at the barrier geometry were calculated and found to correspond to a transition state of the $1\,^1A$ PES (TS2). More exactly, it was characterized as a saddle point of third order, because it has three imaginary frequencies: One associated to the motion along the collinear path of reaction (O–H–C asymmetric stretching) and the other two, which are identical, corresponding to the bending of the O–H–C structure. It can be inferred that the TS2 stationary point governs the abstraction pathway leading from reactants to products of reaction (1).

The reaction pathway for a fixed O–H–C angle equal to the TS2 one (nearly collinear approach) was further analyzed at the CASSCF level. The profile obtained for such pathway is given in Fig. 2. As stated above, TS2 leads directly (without exploring the CH_3OH minimum) to the $OH+CH_3$ asymptote via an abstraction pathway. This pathway passes through a vdW minimum (M2) located in the exit channel of the reaction. The properties of this minimum are shown in Table II.

A better description of the energetics of the $1\,^1A$ PES was obtained by means of the CASPT2 method (Fig. 2). First of all, CASPT2 pointwise calculations on the CASSCF MEP connecting reactants and CH_3OH were carried out. The CASPT2 energies of these points were in all cases below the energy of reactants, even for the CASSCF TS1a and TS1b geometries. Hence, the CASPT2 insertion pathway connecting reactants with the CH_3OH minimum is barrierless. This differs from the CASSCF results (where a barrier 3.8 kcal mol^{-1} high was determined) and is consistent with the experimental findings.[5] Thus, the fact that the overall rate constant for the $O(^1D)+CH_4$ reaction at room temperature is very high and approaches to the gas kinetic limit, together with the observation that is shows a negligible dependence on the temperature, within the 200–350 K interval, suggest that reaction (1) should not present activation energy.[5]

The dissociation pathways of the CH_3OH structure to yield either $OH+CH_3$ (main reaction channel) or CH_3O+H products were also analyzed using the CASPT2 method. As for the CASSCF level, these two possible dissociations evolve without surmounting any energy barrier above products.

As for the insertion type MEP, the CASPT2 pointwise calculations on the CASSCF stationary points of the abstraction pathway [nearly collinear approach of the $O(^1D)$ atom to a C–H bond] yielded energy values below the energy of reactants in all cases. Therefore, the attack of the $O(^1D)$ atom to a C–H bond through a collinear O–H–C arrangement takes place without surmounting any energy barrier along the corresponding collinear pathway. The lack of energy barrier at the CASPT2 level was also observed when computing the CASPT2 energies on the CASSCF structures corresponding to the approach of oxygen to methane for different O–H–C angles. Only for O–H–C attack angles below 90° an energy barrier in the entrance channel of the reaction was observed at the CASPT2 level. Therefore, the CASPT2 $1\,^1A$ PES is quite isotropic at the reactants region for O–H–C angles within the 90°–180° range. This means that although the MEP of the ground PES involved an insertion type reaction path, this particular PES also allows an abstraction reaction path to take place. Nevertheless, due to the existence of the deep CH_3OH minimum on the PES, the contribution of the abstraction mechanism to the reactivity should be expected to be small.

This is consistent with previous results. Thus, QCT calculations on a triatomic analytical representation of the ground PES, which reproduced the main features here established for this surface, showed that reaction (1) mainly proceeded via the insertion mechanism, the abstraction mechanism only accounting for 1%–2% of the reactivity at the usual conditions attained in the experiments.[24] Also, measurements of the energy distribution of the OH product suggested that reaction (1) takes place via an insertion mechanism.[9,11–13]

The presence of a vdW minimum located in the exit channel of reaction (1) for an O–H–C angle of 180° was confirmed at the CASPT2 level.

B. Excited $2\,^1A$ PES

The first excited PES ($2\,^1A$) had not previously been studied to a significant extent. Only in the *ab initio* study of Ref. 22 a preliminary analysis was performed. There, it was reported that in the entrance channel of reaction (1) this PES was much more repulsive than the ground PES ($1\,^1A$). However, recent *ab initio* and dynamic studies about the related $O(^1D)+H_2$ reaction have proved that the role played by the first excited PES ($1\,^1A''$) of the system should not be neglected.[26–32]

Here, we performed two different types of CASSCF calculations on the $2\,^1A$ PES, depending on whether C_1 or C_s symmetries were considered. In the former case, we worked with a state-average CASSCF wave function, because obtaining a pure $2\,^1A$ CASSCF wave function was not possible in most cases, due to its energetic closeness to the ground $1\,^1A$ one. This prevented us from carrying out optimizations and frequency calculations for the $2\,^1A$ PES in C_1 symmetry. On the other hand, when constraining the O, H, C, and H′ atoms to have them in the same plane (i.e., under C_s symmetry), the $2\,^1A$ state converts into the $1\,^1A''$ state. Thus, we recover the advantages of working with ground state wave functions. Preliminary calculations in C_1 symmetry showed that the stationary points and MEP of the $2\,^1A$ surface had C_s symmetry, as had happened for the $1\,^1A$ surface.

The stationary points and MEP obtained at the CASSCF level for the $2\,^1A$ PES are given in Fig. 4 and Table II, and Table B of the supplementary material.[39] The MEP of this PES corresponds to a collinear approach (O–H–C angle of 180°) of the $O(^1D)$ atom to a C–H bond, giving rise to an early transition state (TS1′). Its geometry, energy and harmonic frequencies were computed. However, since these calculations were carried out in C_s symmetry, it was not possible to perform a complete characterization of TS1′, as only frequencies of the A' type could be computed. From these frequencies, it was inferred that TS1′ was an ordinary (first order, one imaginary frequency) saddle point of the PES. Pointwise CASSCF calculations for out-of-plane distortions of the TS1′ geometry always yielded higher energies than that corresponding to TS1′.

TS1′ allows connection of reactants with products via an abstraction pathway, evolving through geometries with collinear O–H–C arrangements. A second stationary point was found along the CASSCF MEP, corresponding to a vdW minimum located in the exit channel of the reaction (M2′). The geometry, energy and harmonic frequencies are the same than the ones for the M2 vdW minimum of the ground $1\,^1A$ PES (cf. in Table II and Table B of the supplementary material[39]). This is due to the degeneracy of the $1\,^1A$ and $2\,^1A$ PESs in the exit channel of the collinear MEP of reaction (1). This situation corresponds to C_{3v} symmetry arrangements of the system.

The CASSCF energy of TS1′ (about 12 kcal mol^{-1}) is much higher than that found for the early collinear TS of the

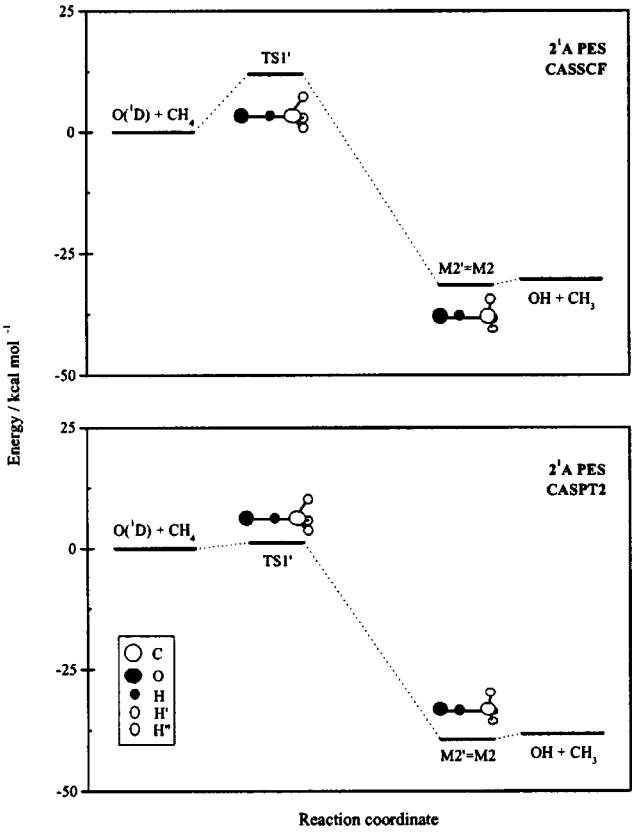

FIG. 4. Schematic representation of the stationary points and connections between them found at the CASSCF and CASPT2 *ab initio* levels for the $2\,^1A$ PES.

$1\,^1A$ PES (TS2). The dependence of the energy barrier on the O–H–C angle was also studied at the CASSCF level for the excited PES, assuming that the O, H, C, and H′ atoms were placed in the same plane (Fig. 3). As stated above, the minimal energy was obtained for a collinear O–H–C structure in this case. When deviating from collinearity the energy barrier steeply increases, so that for the first excited PES the insertion of the $O(^1D)$ into a C–H bond was found to be energetically disfavored. Hence, reactivity over the $2\,^1A$ surface must be expected to occur only via an abstraction mechanism, in contrast with what happens for the $1\,^1A$ surface. Similar results have been obtained for the $O(^1D)+H_2$ reaction.[29,40]

When applying the CASPT2 method to study the excited $2\,^1A$ PES, the main features established at the CASSCF level were reproduced, but the CASPT2 optimal energy for TS1′ was significantly shifted from the CASSCF one. Thus, although the CASPT2 transition state was found to have a collinear O–H–C geometry too, it seemed to occur for a longer O–H distance. In the interest of accurately determining the energy barrier for the excited PES, special pains were taken to obtain the CASPT2 geometry of TS1′. We operated sequentially as follows: (a) a set of 40 CASPT2 points were computed along the reaction coordinate O–H–CH_3, fixing the O–H–C angle to 180° and optimizing the structure of the methyl group for each one of these points at the CASSCF level; (b) the calculated CASPT2 energies were fitted using bicubic splines in terms of the O–H and H–C distances and

the resulting values of these two distances for the CASPT2 TS1′ stationary point were derived employing numerical gradients; (c) the geometry of the methyl group was optimized at the CASSCF level for the R_{OH} and R_{HC} values found and an O–H–C angle equal to 180°. The energy of the final structure was calculated by means of the CASPT2 method (see Table II and Fig. 4).

As mentioned, TS1′ at the CASPT2 level presented a more evident early saddle point character than at the CASSCF level. Thus, R_{OH} is equal to 1.625 and 1.401 Å for the optimal CASPT2 and CASSCF geometries, respectively. Also, a non-negligible energy shift was observed between the CASSCF and CASPT2 saddle points. The high CASSCF energy barrier (12.0 kcal mol^{-1}) is significantly reduced when including the dynamical correlation by means of the CASPT2 method (1.2 kcal mol^{-1}). At this point, it must be noted that the average collision energies usually employed in the experiments on reaction (1) [4.8 kcal mol^{-1},[7,9] 6.5 kcal mol^{-1},[19] and 9.3 kcal mol^{-1} (Refs. 11–18)] are large enough to allow for reactivity on the $2\,^1A$ PES, according to the CASPT2 energy barrier.

In spite of the abovementioned results, no experimental evidence was found of the involvement of the first excited PES on reaction (1). This is probably due to two main reasons: (a) though possible at the usual energies of the experiments, reactivity on the $2\,^1A$ PES should be expected to be significantly smaller than that for the ground surface, as the latter is barrierless and quite isotropic in the entrance channel; (b) it is not easy to experimentally assess the contribution of the excited PES in reaction (1) and specific experiments focused on this problem would be needed. For instance, although a large number of experimental works have been addressed to the elucidation of the energetics of the OH product of reaction (1),[6–13] the highly excited vibrational levels of OH expected to be populated by the abstraction mechanism occurring on the $2\,^1A$ PES have been little analyzed. Such analysis was recently carried out, however, for the analogous $O(^1D)+C_2H_6$ (Ref. 41) and $O(^1D)+C_2H_4$ (Ref. 42) reactions and the findings showed preliminary evidences of the contribution of an abstraction mechanism to the formation of high internally excited OH molecules.

At this point, it is worth considering recent experimental and theoretical investigations reported for the related $O(^1D)+H_2\rightarrow OH+H$ process and its deuterated isotopic variants (see, e.g., Refs. 26–32). From these it has been inferred that, although the major contribution to the reactivity of the system is due to an insertion mechanism evolving through the ground $1\,^1A'$ PES, the low energy barrier presented by the first excited PES ($1\,^1A''$ PES) allows an abstraction mechanism to take place on it. The contribution of this mechanism increases with collision energy and renders OH molecules with specific dynamic properties: pronounced vibrational inversion, low rotational excitation, and backward scattering.

C. Influence of other excited PESs

From the calculations given here, it was inferred that a significant contribution of the excited $2\,^1A$ PES to the reactivity might be expected. The contribution of other excited PESs to the process may be considered to be much less important, since they do not correlate adiabatically with the $OH(X\,^2\Pi)+CH_3$ products. Nevertheless, it might be interesting to estimate the role played by the excited $3\,^1A$ PES for two reasons: (a) it is expected a $1\,^1A-3\,^1A$ avoided crossing for geometries close to C_{3v} symmetry; (b) this avoided crossing might occur once surmounted the barrier of the excited PES, which in principle could be overcome at the usual experimental conditions, because the $2\,^1A$ and $3\,^1A$ PESs are nearly degenerate for geometries close to C_{3v} symmetry at the entrance valley of the reaction. This situation resembles what was described for the related $O(^1D)+H_2$ system, where a non-negligible contribution of the excited $2\,^1A'$ state to the reactivity, due to nonadiabatic interactions with the ground $1\,^1A'$ PES, was reported.[43]

As explained at the beginning of Sec. III, the $1\,^1A-3\,^1A$ avoided crossing arises as a consequence of the crossing between the $1\,^1A_1$ and $1\,^1E$ PESs for C_{3v} symmetry (collinear O–H–C geometries). Therefore, in this work we have just focused on the characterization of the $1\,^1A_1-1\,^1E$ crossing by means of the CASSCF and CASPT2 methods (and the same active space and basis set reported above), in order to investigate the avoided crossing between the $1\,^1A$ and $3\,^1A$ PESs for geometries close to C_{3v} symmetry. Although C_{3v} symmetry could be assumed in the calculations, we carried out them in C_s symmetry because future work is intended to be developed to characterize the $1\,^1A'$ ($1\,^1A$ in C_1) and $2\,^1A'$ ($3\,^1A$ in C_1) PESs around the crossing region. Thus, a state-average A' CASSCF wave function with equal weights of the $1\,^1A'$ and $2\,^1A'$ states was considered in the calculations. A rough picture about the location of the crossing was obtained by analyzing the energy difference between the $1\,^1A'$ and $2\,^1A'$ roots of the state-average CASSCF solution. This was done for all geometries previously computed when studying the collinear $O–H–CH_3$ pathway connecting reactants with products through the $1\,^1A$ PES. The point with the least energy difference between both roots was taken as a first approximation of the crossing geometry. Afterwards, a set of 40 CASPT2 and CASSCF energies was calculated for several R_{OH} and R_{CH} distances around that geometry, fixing the O–H–C angle to 180° and taking the CH_3 structure from a pure $1\,^1A'$ CASSCF optimization calculation. A 2D map of the differences between the $1\,^1A'$ and $2\,^1A'$ energies was determined by fitting a bicubic splines expression to the calculated energies and, by numerical differentiation, the point with minimal energy difference was found. The geometry of this point was taken as the lowest energy crossing structure between the $1\,^1A_1$ and $1\,^1E$ PESs (see Table III).

For both the CASSCF and CASPT2 calculations, the $1\,^1A_1-1\,^1E$ PESs crossing is observed to occur once the early barrier for the excited PES is surmounted, which has been previously calculated (see TS1′ in Table II). Thus, the R_{OH} values found for the crossing and the barrier were 1.081 Å (CASSCF) and 1.073 Å (CASPT2), and 1.401 Å (CASSCF) and 1.625 Å (CASPT2), respectively. Because the energy barrier for the $1\,^1E$ PES is only 1.2 kcal mol^{-1} high (at the CASPT2 level), the crossing region might be accessed at the usual experimental conditions when the sys-

TABLE III. Properties of the lowest energy crossing structure between the $1\ ^1A_1$ and $1\ ^1E$ PESs.[a]

	R_{OH}/Å	R_{HC}/Å	$R_{H'C}$/Å	$R_{H'C}$/Å	∠CHO/°	∠H′CH/°	∠H″CH/°	ΔE/kcal mol^{-1} [b]	E/kcal mol^{-1} [c]
CASSCF	1.081	1.280	1.094	1.094	180.0	101.7	101.7	0.1	6.4
CASPT2	1.074	1.307	1.090	1.090	180.0	101.0	101.0	0.1	−15.6

[a]See Fig. 2 for the internal coordinates definition. See text.
[b]Energy difference between the PESs at the lowest energy crossing geometry found.
[c]Energy of the $1\ ^1A$ PES at the crossing geometry mentioned above. Energy referred to reactants.

tem evolves on this PES. This means that, in case that small distortions of the collinear O–H–C arrangement leading to C_s or C_1 geometries occur, the avoided crossing region will be explored, where significant nonadiabatic interactions might be expected between the $1\ ^1A'$ ($1\ ^1A$ in C_1) and $2\ ^1A'$ ($3\ ^1A$ in C_1) PESs. As a consequence, the excited $3\ ^1A$ surface might contribute to the reactivity of reaction (1) for geometries close to C_{3v} symmetry, although it does not adiabatically correlates with the $OH(X\ ^2\Pi)+CH_3$ products.

IV. SUMMARY AND CONCLUSIONS

The two potential energy surfaces ($1\ ^1A$ and $2\ ^1A$ PESs) adiabatically correlating the reactants and products asymptotes of the title reaction were studied by means of the CASSCF and CASPT2 methods. A full valence active space and a large basis set [6-311G(2*df*,2*pd*)] were employed.

At the highest *ab initio* level considered, the minimum energy path determined for the ground PES ($1\ ^1A$) evolved through the barrierless insertion of the $O(^1D)$ atom into a C–H bond of methane. The $OH+CH_3$ products arise from the dissociation of the CH_3OH intermediate formed. However, it was also found that reaction (1) may alternatively occur via an abstraction pathway through nearly collinear O–H–C geometries (without involving the CH_3OH minimum).

Reactivity over the excited $2\ ^1A$ PES was found to proceed only via an abstraction pathway. The energy barrier calculated for such process at the CASPT2 level is low enough (1.2 kcal mol^{-1}) to expect that the $2\ ^1A$ PES plays a non-negligible role in the reaction, even at the usual conditions of the experiments. Although no experimental evidence was found yet of such a situation, we believe that specific experiments different from those already reported in the literature should be required in order to assert it.

Finally, the avoided crossing between the $1\ ^1A$ and $3\ ^1A$ PESs was also investigated, the latter surface correlating with the excited $OH(A\ ^2\Sigma^+)$ product. The features found for the crossing are such that it might be expected a non-negligible contribution of the $3\ ^1A$ PES to reaction (1), as a result of the nonadiabatic interaction with the $1\ ^1A$ PES. However, dynamic calculations on reaction (1), accounting for nonadiabatic couplings between PESs, will be required in order to unravel this point.

ACKNOWLEDGMENTS

This work was supported by the ''Dirección General de Enseñanza Superior'' of the Spanish Ministry of Education and Culture through Project Nos. PB98-1209-C02-01 and -02, and also by the ''Dirección General de Investigación'' of the Spanish Ministry of Science and Technology through Project Nos. BQU2002-04269-C02-01 and -02, and BQU2002-03351. Financial support from the ''Generalitat de Catalunya'' (Autonomous Government of Catalonia) Ref. 2001SGR 00041 is also acknowledged. J.H. thanks the CIRIT from the ''Generalitat de Catalunya'' for a predoctoral research grant. The authors are also grateful to the ''Center de Supercomputació i Communicacions de Catalunya (C^4-CESCA/CEPBA)'' for computer time made available.

[1] M. W. Chase, Jr., C. A. Davies, J. R. Downey, Jr., D. J. Frurip, R. A. McDonald, and A. N. Syverud, J. Phys. Chem. Ref. Data **14**, 1 (1985).
[2] J. R. Wiesenfeld, Acc. Chem. Res. **15**, 110 (1982).
[3] P. Warneck, *Chemistry of the Natural Atmosphere* (Academic, San Diego, 1988).
[4] E. B. Burnett and C. R. Burnett, J. Atmos. Chem. **21**, 13 (1995).
[5] R. Atkinson, D. L. Baulch, R. A. Cox, R. F. Hampson, Jr., J. A. Kerr, M. J. Rossi, and J. Troe, J. Phys. Chem. Ref. Data **28**, 191 (1999), and references therein.
[6] A. C. Luntz, J. Chem. Phys. **73**, 1143 (1980).
[7] P. M. Aker, J. J. A. O'Brien, and J. J. Sloan, J. Chem. Phys. **84**, 745 (1986).
[8] S. G. Cheskis, A. A. Iogansen, P. V. Kulakov, I. Yu. Razuvaev, O. M. Sarkisov, and A. A. Titov, Chem. Phys. Lett. **155**, 37 (1989).
[9] C. R. Park and J. R. Wiesenfeld, J. Chem. Phys. **95**, 8166 (1991).
[10] Y. Rudich, Y. Hurwitz, G. J. Frost, V. Vaida, and R. Naaman, J. Chem. Phys. **99**, 4500 (1993).
[11] M. González, J. Hernando, R. Sayós, M. P. Puyuelo, P. A. Enríquez, J. Guallar, and I. Baños, Faraday Discuss. **108**, 453 (1997).
[12] S. Wada and K. Obi, J. Phys. Chem. A **102**, 3481 (1998).
[13] M. González, M. P. Puyuelo, J. Hernando, R. Sayós, P. A. Enríquez, J. Guallar, and I. Baños, J. Phys. Chem. A **104**, 521 (2000).
[14] M. Brouard, S. P. Duxon, and J. P. Simons, Isr. J. Chem. **34**, 67 (1994).
[15] M. Brouard and J. P. Simons, in *The Chemical Dynamics and Kinetics of Small Radicals, Part II*, edited by K. Liu and A. Wagner (World Scientific, Singapore, 1995), p. 795.
[16] M. Brouard, H. M. Lambert, J. Short, and J. P. Simons, J. Phys. Chem. **99**, 13571 (1995).
[17] M. Brouard, H. M. Lambert, C. L. Russell, J. Short, and J. P. Simons, Faraday Discuss. **102**, 179 (1995).
[18] J. P. Simons, J. Chem. Soc., Faraday Trans. **93**, 4095 (1997).
[19] J. J. Lin, J. Shu, Y. T. Lee, and X. Yang, J. Chem. Phys. **113**, 5287 (2000).
[20] T. Suzuki and E. Hirota, J. Chem. Phys. **98**, 2387 (1993).
[21] R. Schott, J. Schlütter, M. Olzmann, and K. Kleinermanns, J. Chem. Phys. **102**, 8371 (1995).
[22] H. Arai, S. Kato, and S. Koda, J. Phys. Chem. **98**, 12 (1994).
[23] M. González, J. Hernando, I. Baños, and R. Sayós, J. Chem. Phys. **111**, 8913 (1999), and references therein.
[24] M. González, J. Hernando, M. P. Puyuelo, and R. Sayós, J. Chem. Phys. **113**, 6748 (2000).
[25] R. Sayós, J. Hernando, M. P. Puyuelo, P. A. Enríquez, and M. González, Phys. Chem. Chem. Phys. **4**, 288 (2002).
[26] Y.-T. Hsu, J.-H. Wang, and K. Liu, J. Chem. Phys. **107**, 2351 (1997).
[27] M. Alagia, N. Balucani, L. Cartechini, P. Casavecchia, E. H. van Kleef, G. G. Volpi, P. J. Kuntz, and J. J. Sloan, J. Chem. Phys. **108**, 6698 (1998).
[28] Y.-T. Hsu, K. Liu, L. A. Pederson, and G. C. Schatz, J. Chem. Phys. **111**, 7931 (1999).
[29] G. C. Schatz, A. Papaioannou, L. A. Pederson, L. B. Harding, T. Hollebeek, T. S. Ho, and H. Rabitz, J. Chem. Phys. **107**, 2340 (1997).

[30] K. Drukker and G. C. Schatz, J. Chem. Phys. **111**, 2451 (1999).
[31] S. K. Gray, C. Petrongolo, K. Drukker, and G. C. Schatz, J. Phys. Chem. A **103**, 9448 (1999).
[32] F. J. Aoiz, L. Bañares, M. Brouard, J. F. Castillo, and V. J. Herrero, J. Chem. Phys. **113**, 5339 (2000).
[33] L. Salem and C. Rowland, Angew. Chem., Int. Ed. Engl. **11**, 92 (1972).
[34] B. O. Roos, Adv. Chem. Phys. **69**, 399 (1987).
[35] K. Andersson and B. O. Roos, in *Modern Electronic Structure Theory*, edited by D. R. Yarkony (World Scientific, Singapore, 1995), Part I, p. 55.
[36] MOLCAS, Version 4.1, K. Andersson, M. R. A. Blomberg, M. P. Fülscher *et al.* (Lund University, Sweden, 1998).
[37] M. J. Frisch, J. A. Pople, and J. S. Binkley, J. Chem. Phys. **80**, 3265 (1984).
[38] T. H. Dunning, Jr., J. Chem. Phys. **90**, 1007 (1989).
[39] See EPAPS Document No. E-JCPSA6-119-305342 for the *ab initio* and experimental geometries and harmonic frequencies of the reactants and products molecules, and for the CASSCF harmonic frequencies of the stationary points of the 1 ^1A and 2 ^1A PESs. A direct link to this document may be found in the online article's HTML reference section. This document may also be retrieved via the EPAPS homepage (http://www.aip.org/pubservs/epaps.html) or from ftp.aip.org in the directory /epaps/. See the EPAPS homepage for more information.
[40] T. S. Ho, T. Hollebeek, H. Rabitz, L. B. Harding, and G. C. Schatz, J. Chem. Phys. **105**, 10472 (1996).
[41] M. González, M. P. Puyuelo, J. Hernando, R. Sayós, P. A. Enríquez, and J. Guallar, J. Phys. Chem. A **105**, 9834 (2001).
[42] M. González, M. P. Puyuelo, J. Hernando, R. Martínez, R. Sayós, and P. A. Enríquez, Chem. Phys. Lett. **346**, 69 (2001).
[43] M. R. Hoffmann and G. C. Schatz, J. Chem. Phys. **113**, 9456 (2000).